A Mathematical Model of Oscillatory Chemicurrents in Oxyhydrogen Interaction with Pt/GaP Nanostructures

BY

SONGYUN LIU

B.Eng., Hefei University of Technology, 2012

THESIS

Submitted as partial fulfillment of the requirements

for the degree of Master of Science in Materials Engineering

in the Graduate College of the University of Illinois at Chicago, 2016

Chicago, Illinois

Defense Committee:

Eduard Karpov, Chair and Advisor, CME

Michael J. McNallan, CME

Didem Ozevin, CME

Acknowledgements

Countless thanks to my advisor, Professor Eduard Karpov. This thesis work was only possible through your patient and dedicated guidance. Thank you so much for offering your encouragement, expertise, and support continuously.

The author wants to thank Professor Lewis Wedgewood for fruitful discussion. Thank you for your valuable comments and suggestions.

Also, I must express my sincerest gratitude to my committee members, Professors Didem Ozevin and Michael J. McNallan for taking time out from their schedules to share advice and guidance. All your efforts make this work the best it can be.

To my family and friends, I shall express my deepest thanks for your unwavering love and support. I could not come this far without you, and I know you will always be with me. Special thanks to my wife Jade He, whose unequivocal love and encouragement carried me through the life on a foreign land.

TABLE OF CONTENTS

LIST OF TABLES

LIST OF FIGURES

SUMMARY

Nonlinear dynamics is a critical branch in the realm of heterogeneous catalysis. People care about the kinetics of chemical reactions, especially the catalytic oxidation of hydrogen on platinum, the very first catalytic reaction in the history. The observed oscillating chemicurrent signals indicate that the system undergoes transitions between several stable states, and their dynamical behavior is absolutely nonlinear. Therefore, we propose a reaction mechanism and use numerical simulation to qualitatively reproduce the behavior obtained from experiments. Specifically, we first explore two classic and well-established chemical oscillators where the oscillatory dynamics are similar to our case. A discussion of their dynamics, specifically the potential bifurcation scenario, is provided. With this guidance, a mathematical model is set, and desired dynamic features have been laid out. Furthermore, we map out the stability phase diagram to better understand the dynamics of our proposed model.

1 INTRODUCTION

1.1 Nonlinear Dynamics of Oscillating Heterogeneous Reactions

Ever since the first report of rate oscillation from experimental observation [6], this attractive phenomenon has soon captured the attention of scientists. Even before that, the oscillating reactions in homogeneous liquid system has been recognized for decades: Belousov–Zhabotinskii (BZ) reaction [15] is perhaps the most remarkable system both for its spectacular behavior and the story behind it [37]. The overall BZ reaction can be described by Eq. 1. The feedback mechanism causing the autocatalysis leads to the concentration variation spatially. Fig.1. is the image of Belousov–Zhabotinskii reaction. The variation in color is due to spatial differences in chemical composition, which varies throughout time and space.

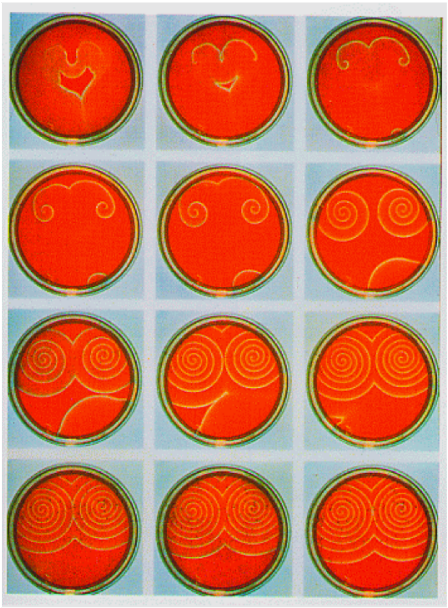

Figure 1: Spiral waves of chemical activity in a shallow dish of the BZ (Belousov–Zhabotinskii) reaction. Reproduced with the permission from Scientific American Ref.[41].

$$3CH_2(CO_2H)_2 + 4BrO_3 \rightarrow 4Br + 9CO_2 + 6H_2O \tag{1}$$

Beside the BZ reaction, heterogeneously catalyzed carbon monoxide oxidation [13, 7, 10] and NO reduction on platinum [23, 24] are two typical reactions which have been subjected to thoroughly investigations for their oscillatory behaviors. Taking catalytic CO oxidation as an example, the establishment of the mechanism [11, 16] follows Langmuir–Hinshelwood (L-H) scheme presented by the following Eq. 2. The symbol "*" here denotes an available adsorption vacant site on platinum surface.

$$\begin{aligned} \mathrm{CO} + * &\rightleftharpoons \mathrm{CO_{ad}} \\ \mathrm{O_2} + 2* &\rightarrow \mathrm{O_{ad}} \\ \mathrm{O_{ad}} + \mathrm{CO_{ad}} &\rightarrow \mathrm{CO_2} + 2* \end{aligned} \tag{2}$$

The arising oscillation is due to the surface phase transition caused by the variation of coverage of CO on the Pt(110). This proposed mechanism was first confirmed by the direct evidence obtained by in situ low-energy electron diffraction (LEED) experiment [12]. The work function measurements showed the coupling between the oscillatory rate and periodic structural changes during the surface reaction. An illustration of this mechanism can be viewed in Fig. 2. Specifically, it begins with the more active 1×1 CO-covered surface and when CO concentration drops to its critical value due to surface reaction, it reconstructs into a less active 1×2 surface. Since O_2 is highly structure sensitive to its adsorbed surface and correspondingly has two different sticking coefficients on two phases, this leads to the variation in adsorbed O_2 coverage. Therefore, the cyclic change of the surface concentration gives the overall oscillatory activity.

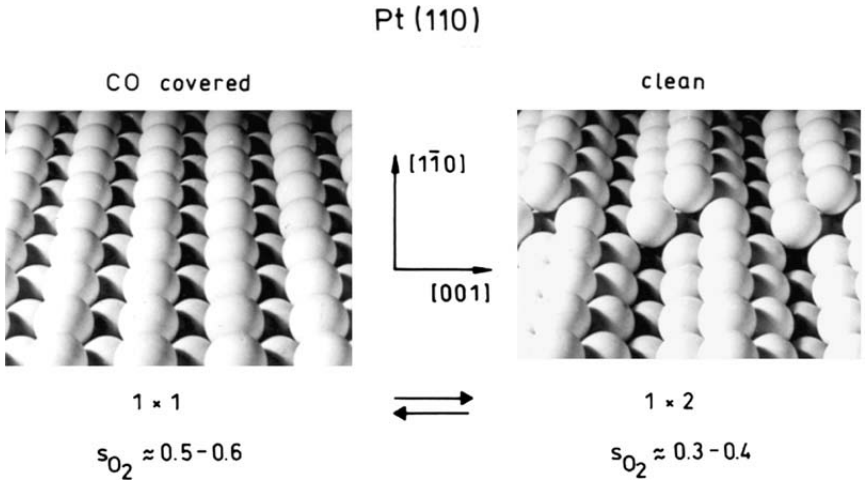

Figure 2: Illustration of phase transition model. The CO induced a $1\times1 \rightleftharpoons 1\times2$ surface phase transition of Pt(110) serving like an activity switch between high and low. Reproduced with the permission from Ref.[22]. Copyright © 2008 Elsevier B.V. All rights reserved.

Dynamics is the main characteristic of a chemical system. One of the most interesting topics lies in the origin of the self-oscillation processes. Generally, oscillations in reaction systems that far from equilibrium fall into the category of non-equilibrium thermodynamics. Such systems are usually called "dissipative structures" [28]. People realized these fascinating behaviors observed in experiments represent their actual dynamic processes [35]. The area of nonlinear dynamics has then been built upon its connection with the study of heterogenous catalysis. A plenty of researches have been carried out on different reaction systems [34, 23]. Several issues of journals focusing on the nonlinear dynamics on catalytic surfaces have been published [9, 36]. The nonlinear dynamics itself as a powerful tool has also been applied to various biological studies [1, 42, 17], and an interesting example is the study of pattern evolution in animals, which has been first brought out by Turing and his study on morphogenesis [38]. The study of nonlinear dynamics is not only to improve our understanding on weird

phenomena like chemical oscillations, but to shed light on how we can take advantage of the underlying mechanism to control these reaction under the condition of a real-life catalysis.

1.2 Motivation and the Goals

Even though the catalytic oxidation of hydrogen on platinum surface has been intensively studied with numerous hypothetical models being proposed [20, 43, 39, 33, 21], very small amount of works are based on the mechanistic aspect of oscillatory kinetics and the real reaction mechanism is still lacking an agreement. Besides, most of the previous research were carried out on the single crystal surface under low temperature (i.e. it usually below 170K, which is desorption temperature of water molecule) while our experimental setup is with polycrystalline catalyst at around 450K, therefore more close to a "real catalyst" operation condition.

The purpose of this thesis is, firstly, to use the knowledge of nonlinear dynamics to perform analysis on the dynamical behaviors of certain classic catalytic chemical systems: 1) Lotka-Volterra model, and 2) Brusselator model. Both of them possess typical oscillatory dynamics which are similar to our case. Then, we specifically investigate the hydrogen oxidation reaction and provide a mathematical model to describe the unusual nonlinear phenomena obtained from our detected current signals. We hope to generate this simple model to help us better understand this long-lasting mechanistic problem.

2 BACKGROUND AND RELATED WORK

2.1 Chemicurrent Detection with Metal-semiconductor Structures

The detection of excited charge carrier transfer through a thin-film metal-semiconductor structures has gained much attention due to the promising application in energy conversion recently[29, 32, 19]. Typically, we refer this metal-semiconductor junction as a Schottky diode. The term "chemicurrent" [30] was first coined to describe the observed electron flow from Cu film all the way through Schottky structure to the external circuit during exothermic adsorption of hydrogen on Cu surfaces. The current is based on a non-adiabatic(non-equilibrium) electron–hole pair creation. Specifically, hot electrons or holes with excess energies higher than the barrier height Φ can be detected in both types of semiconductors. Detailed illustrations about the principle of hot charge carriers are depicted in Fig. 3.

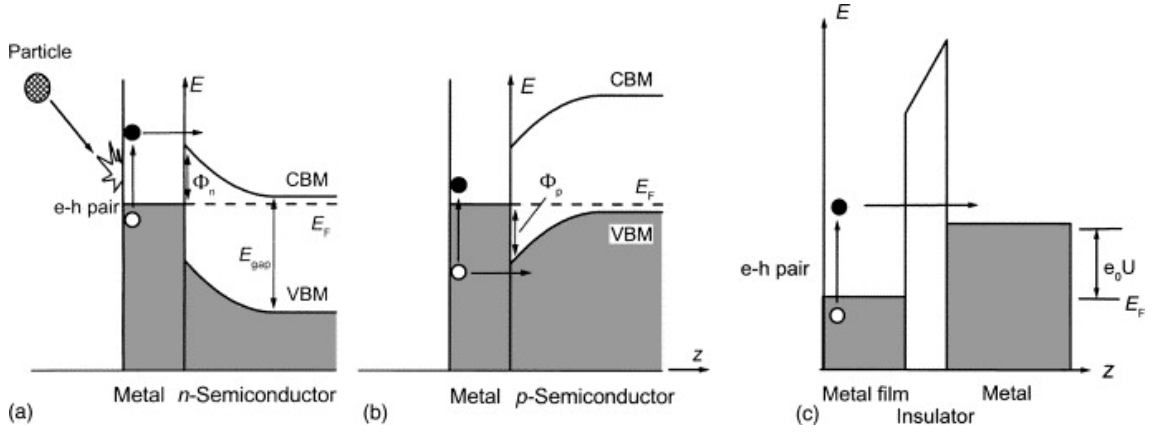

Figure 3: Schematic representation of the chemicurrent sensing with the (a) n-type Schottky diode, (b) p-type Schottky diode, and (c) Metal-Insulator-Metal tunnel structure. Ballistically transportation of hot charge carriers through the surface to the interface when excess energy are greater than barrier height. The Fermi level of the metal is indicated as E_{F}. Reproduced with permission from Ref. [31]. Copyright © 2002 Elsevier B.V. All rights reserved.

2.2 Mathematical Descriptions of Oscillatory Behavior

All oscillating reactions possess two features: nonlinearity and feedback. The oscillatory behavior can be generally described as the recurrence of reactants and products to reach local maxima with time. To get information of species concentration in a system, we can solve the kinetic model of that system.

Commonly, it is the reaction mechanism that governs the rate of a catalytic reaction, i.e. a certain step of elementary reactions (sometimes referred to as simple reactions). These steps in turn are under the control of parameters such as the concentrations (i.e. partial pressures p_j) of all the reactants in gas phase and temperature T. Specifically, the adsorbed species are usually assumed to be randomly distributed over the catalytic metal surface, and their concentrations (fractional coverages) θ_i are treated with a mean-field approximation [14] so that the reaction rate (number of molecules r formed per unit time) is given by

$$\frac{\mathrm{d}n_r}{\mathrm{d}t} = f(\theta_i, T) \tag{3}$$

whereby the fractional coverages θ_i are in turn determined by a general framework of ordinary differential equations (ODEs) of the type [14]

$$\frac{\mathrm{d}\theta_i}{\mathrm{d}t} = f_i(p_i, \theta_i, T) \tag{4}$$

Then, heat and mass balance are taken into consideration as additional constrains to complete the model.

Throughout this thesis, we should bear in mind that we simply assume the reaction is spatially homogeneous on the catalytic surface and we ignore the factor of pattern formation, therefor we study the mechanism in regards to a point model of ODEs which represents the local variation of kinetics. Under steady state condition, with all the external parameters being kept fixed, usually a constant rate can be expected, i.e., $\mathrm{d}\theta_i/\mathrm{d}t = 0$. By the mathematical definition, the name, nonlinear dynamics, reflects the existence of nonlinearity in these coupled ODEs. Therefore, due to this feature of the quoted differential equations, the kinetics may – given certain variations of parameters – become oscillatory or even chaotic.

Since our main interest here is to figure out what makes the transition from a stationary current to an oscillatory one, Eq. 4 can be applied to a systematic analysis of different solutions with the help of bifurcation theory [18]. For example, in a system with two variables, only a few amount of bifurcations are possible. With the phase plane technique, we can relate two situations with respect to fixed points or limit cycles. Fig. 4 gives a review of possible bifurcations in 2-D. Given the conditions with more variables, more complex behaviors will be formed, such as mixed-mode oscillations.

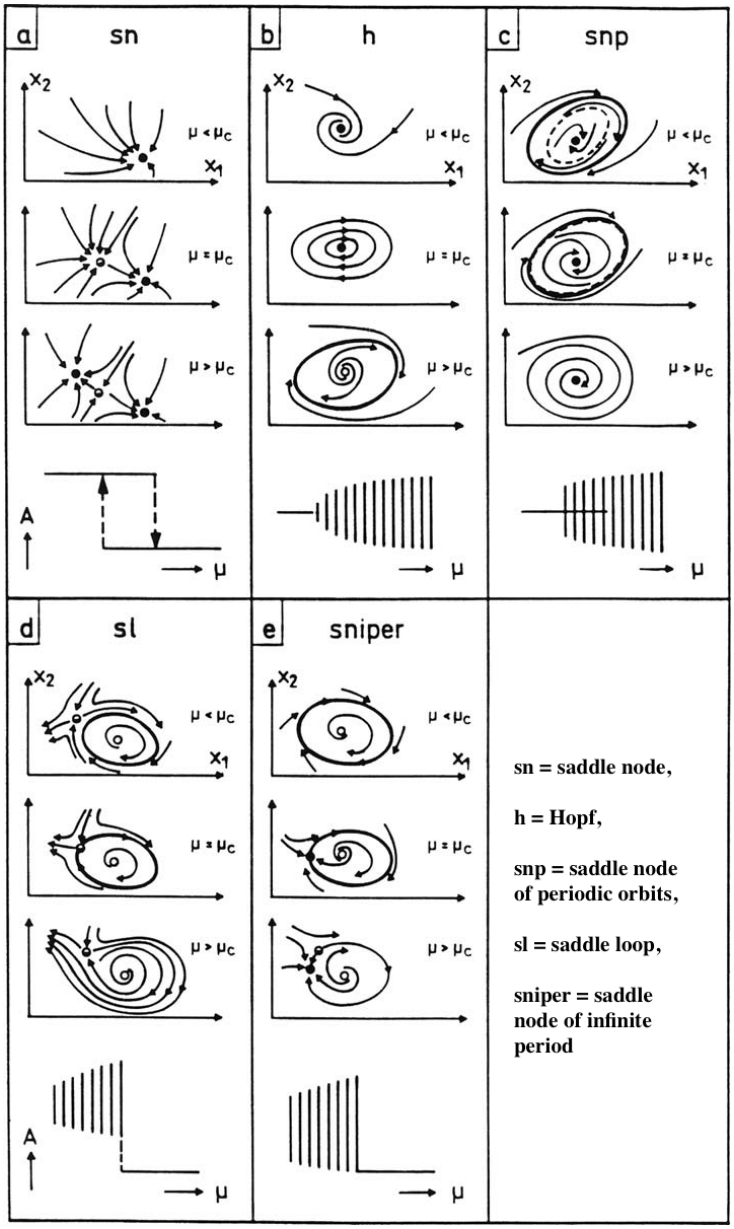

Figure 4: Possible types of bifurcation behaviors which can occur in a system dependent on by two variables, i.e. in a system described by two coupled ODEs. Illustrated are the diagrams in phase space as the bifurcation parameter μ is swept across the bifurcation point, μ_c, and the experimentally observable behavior of some signal A, oscillation amplitudes, during this sweep. Specifically, filled circles are represented a stable steady state (i.e. stable node), half-filled circles a saddle point, and open circles an unstable steady state (i.e. unstable node), respectively. The abbreviations used for different bifurcation scenarios are provided along with this schematic. Reproduced Reproduced with the permission from Ref.[22].

2.3 Hydrogen Oxidation on Catalytic Surfaces

It was in July 1823, Döbereiner, a chemistry professor, told his friend Goethe that he has observed a fascinating phenomena: hydrogen burns rapidly "by mere contact" with platinum. Later on, Berselius was the first to introduce the concept of catalysis into chemistry to categorize these types of reactions [8]. We can almost safely say that hydrogen oxidation is the beginning of modern catalytic chemistry, not to mention its fundamental significance in surface chemistry. As was mentioned in the previous section, numerous studies of this reaction have been done, and regardless the simplicity this seems to be, its underlying mechanism is still not clear. Due to the difference of surface temperature and the ratio of H_2/O_2 mixture, the reaction can occur either homogeneously (gas phase) or heterogeneously (gas-solid interface). Since we mainly focus on heterogeneous reaction, here we present a summarization of possible elementary reactions over the platinum surface by Williams et al. [40]. Note that the letter "s" within parentheses represents the surface adsorbed species. Beside platinum, this reaction has also been studied on other noble metal like Pd, Rh, and Ir, and even in the liquid phase within the field of electrochemistry.

Reaction No.	Reaction
1	$H(s) + O(s) \leftrightarrow OH(s) + Pt$
2	$OH(s) + Pt \leftrightarrow H(s) + O(s)$
3	$H(s) + OH(s) \leftrightarrow H_2O(s) + Pt$
4	$H_2O(s) + Pt \leftrightarrow H(s) + OH(s)$
5	$2OH(s) \leftrightarrow H_2O(s) + O(s)$
6	$H_2O(s) + O(s) \leftrightarrow 2OH(s)$
7	$H_2 + 2Pt \leftrightarrow 2H(s)$
8	$2H(s) \leftrightarrow H_2 + 2Pt$
9	$O_2 + 2Pt \leftrightarrow 2O(s)$
10	$2O(s) \leftrightarrow O_2 + 2Pt$
11	$H_2O + Pt \leftrightarrow H_2O(s)$
12	$H_2O(s) \leftrightarrow H_2O + Pt$
13	$OH(s) \leftrightarrow OH + Pt$

Table 1: A summary of possible elementary reactions for heterogeneous hydrogen oxidation over platinum surface

The first experimental observation of kinetic self-oscillation of catalytic oxidation of hydrogen was found on pellet with 0.4% Pt on γ-Al_2O_3 in 1972 [6], and then similar behavior was also observed on nickel foil [4], platinum wire [3], and platinum foil [5]. Ertl et al. also studied this reaction specifically on its spatiotemporal traveling waves [33, 21]. In all, none of these studies have reported a mixed-mode oscillation. In this work, we will present our model to describe this observed behavior.

3 EXPERIMENT AND DATA

3.1 Experimental Setup

The experimental setup in this work is presented in Fig. 5. This system consists of a SRS RGA Model 200 mass-spectrometer, an ultra high vacuum (UHV) chamber which is our central part in this study where hydrogen oxidation takes place, a PTC 10 multichannel programmable temperature controller, a Keithley 2400 source meter, a TURBOLAB 80 vacuum pumping system, and three types of absolute pressure transducers, which are MKS Types 722A, 722B, and 626.

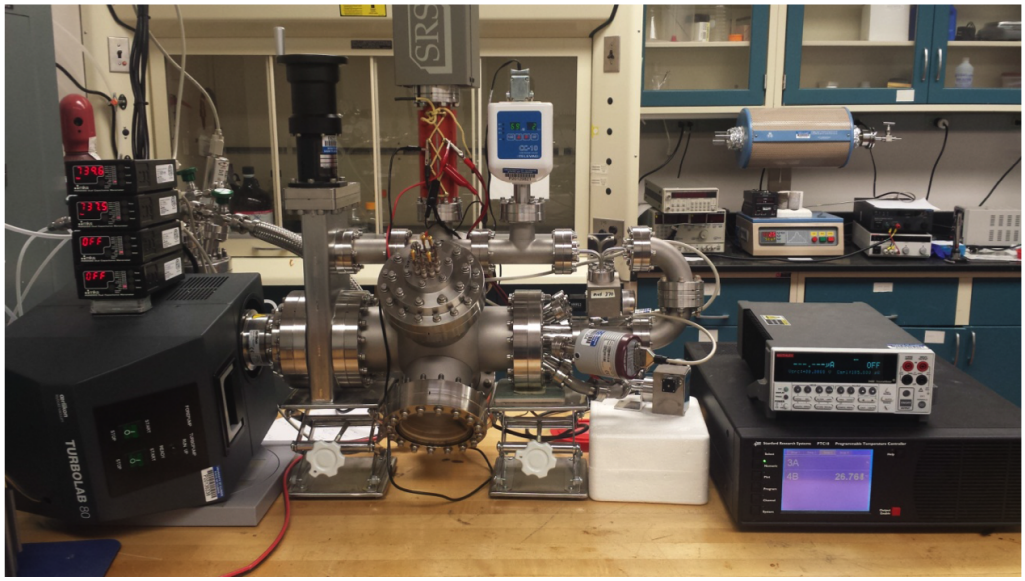

Figure 5: The experimental setup for chemicurrent measurement (Photo's courtesy of Mohammad A. Hashemian)

3.2 Sample Preparation

Our hot electron harvester user a continuous nano-film of platinum deposited on a planar n-GaP semiconductor to fabricate a Schottky junction. This heterojunction nanostructure,

as we mentioned in the previous section 2.1, can allow the internal emission of chemically induced hot electrons over the Schottky barrier ballistically. On its back side, it follows by a deposition of pure indium to form the Ohmic contact. The illustration of this planar structure is shown in Fig. 6. To be specific of the fabrication procedure, a Pt/n-GaP planar nanostructure was fabricated by physical vapor deposition (PVD) process of 0.9999 pure 15 nm platinum film through a 15 nm$\times$2.3 cm^2 area opening onto polished side of a 20$\times$18$\times$0.5 mm^3 n-type gallium phosphide substrate of 0.03 Ω·cm resistivity. The reverse side of the GaP substrate is unpolished and used to support a wide area Ohmic contact made with thermal (593 K) infusion of pure indium. Then, a continuous 40~50 μm capping layer was formed through 10s exposure to a tin melt at 643 K.

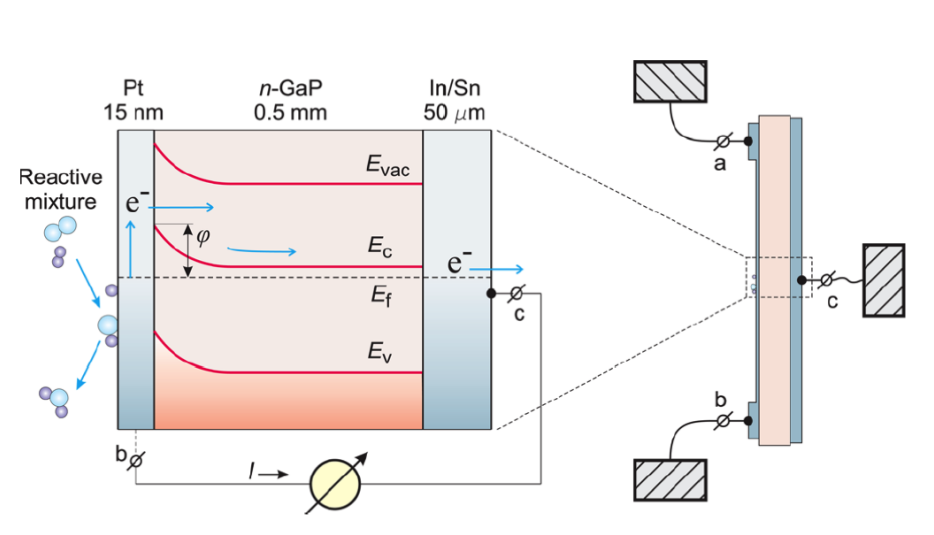

Figure 6: Illustration on the left shows a side cross-section of our Pt/n-GaP Schottky nanostructure. ϕ: Schottky barrier height, E_{vac}: vacuum level, E_c: conduction-band bottom, E_f: Fermi energy, and E_v: valence band top. The schematics on the right depicts our mounted sample without the help of a sample holder(by using thin conductive wires suspended in the UHV chamber in order to minimize heat exchange with any other objects). Reproduced with permission from Ref. [19]. Rights managed by AIP Publishing LLC.

3.3 Chemicurrent Measurement

Chemically induced currents through the Pt/n-GaP nanostructure were measured for the reactive 0.2 Torr mixtures, with a ratio of $H_2/O_2 \approx 2:1$, at surface temperatures of 450 K. Sample surface was outgassed under 10^{-7} Torr vacuum for 20 min before the injection of a gas mixture. Current magnitude measurements were taken as the H_2O turnover rate reaches a maximal read on the mass spectrometer. Nano-film heating was initiated once completion of the mixture injection was completed. The heater kept a constant surface temperature at 450 K throughout the whole experiment. Results for detected current signals are provided in the following Fig. 7. In the Fig. 7_a and 7_b_1, quintessential current profiles are provided with which there is a minor difference in their set-up conditions. A sharp peak of decaying current was detected after the injection of the gas mixture in both experiments, but under the condition of Fig. 7_b_1, the current was bouncing back to reach a maxima doubled the read in the Fig. 7_a. However, it is clear that this type of oscillation mode is reproducible. It is worth noting that we also recorded consecutive current profiles in a longer time span for Fig. 7_b case as shown in Fig. 7_b_2 to7_b_4. At 16.3 min, the analytical chamber was starting a evacuation, therefore there is a clear shift downward in current value, and then the oscillating behavior featured in Fig. 7_a and 7_b_1 came up again except their shape has flipped up side down. It seems that this type of oscillating behavior has its own periodicity. Fig. c_1 and c_2 are the high resolution current profiles corresponding to the region of interest which the oscillations were present.

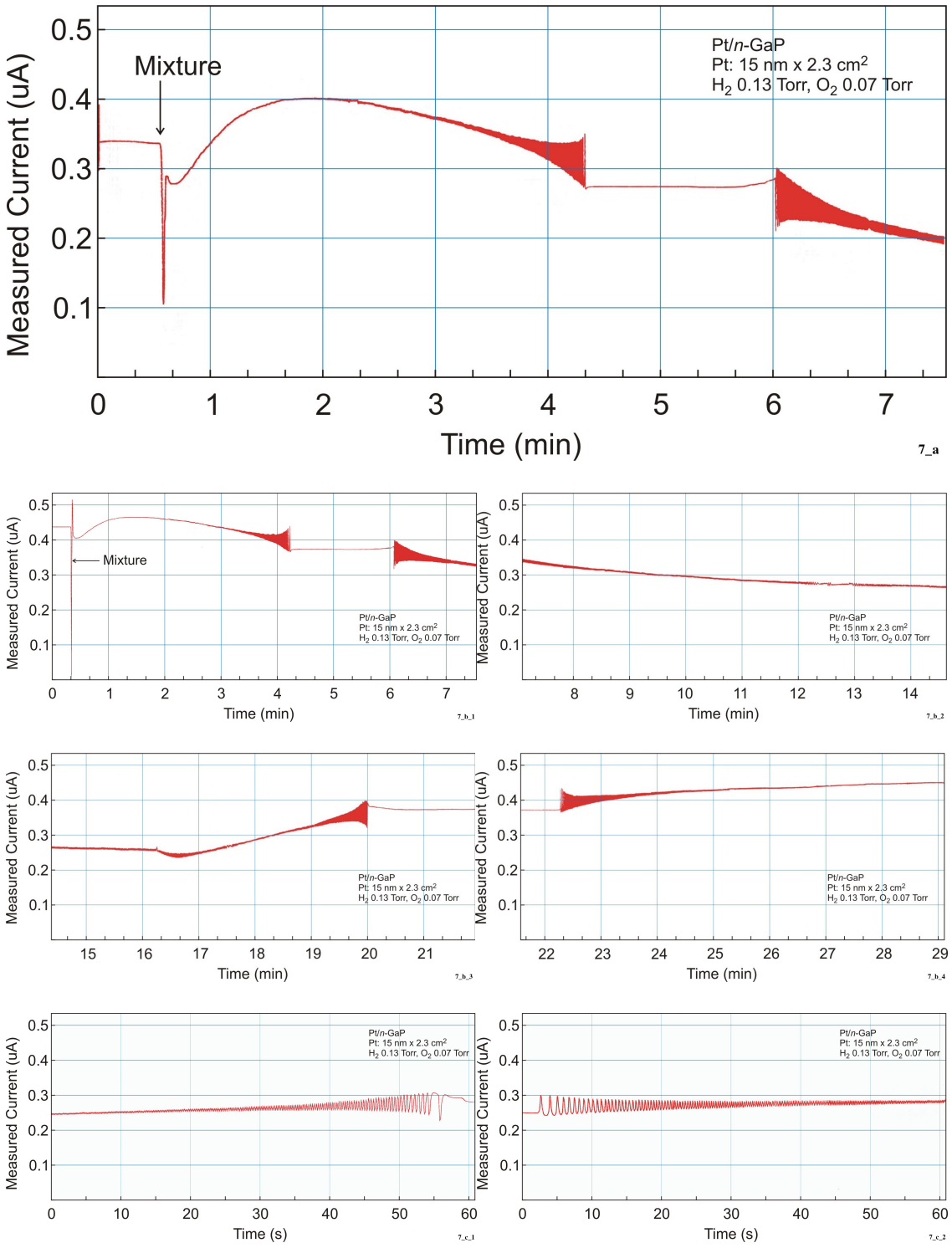

Figure 7: Measured chemicurrent profiles: a) a quintessential oscillating current profile from experiment; b) a whole frame of the detected current in longer time span with a continuous evacuation at 16.3 min; c) high resolution profiles of the region of interest.

In the next section, we will provide a model analysis from a mechanistic perspective for the origin of this mixed-mode oscillation.

4 MATHEMATICAL MODEL ANALYSIS

In this section, we first provide an analysis on two famous models named Lotka-Volterra model (popularly known as the "predator-prey" model) and the Brusselator model. The analysis shows how to establish a mathematical model based on the chemical reactions. Then this paper will present our proposed model to describe our observed behavior.

4.1 Lotka-Volterra Model

As shown below in Eq. 5, the Lotka-Volterra model [25] can represent certain elementary chemical processes:

$$\begin{gathered} step\,1 : A + \mathrm{X} \rightarrow 2\mathrm{X} \\ step\,2 : \mathrm{X} + \mathrm{Y} \rightarrow 2\mathrm{Y} \\ step\,3 : \mathrm{Y} \rightarrow B \\ overall : A \rightarrow B \end{gathered} \tag{5}$$

Notice that the reaction is carried out by setting the concentration of A constant, and the product B will not affect the reaction rate. Therefore, the only relevant reactant species are intermediates X and Y. The differential rate expression for x and y can be then described by two coupled ODEs as shown in Eq. 6.

$$\begin{aligned} \tfrac{\mathrm{d}x}{\mathrm{d}t} &= ax - bxy \\ \tfrac{\mathrm{d}y}{\mathrm{d}t} &= -cy + dxy \end{aligned} \tag{6}$$

As an example, let us set dimensionless parameters a=1, b=2, c=3, d=4; the nullclines can be found analytically by plotting Eq. 7.

$$\begin{cases} ax - bxy = 0 \\ \\ -cy + dxy = 0 \end{cases} . \tag{7}$$

The nullclines are used for determining global behavior of solutions. We can have the fixed points $\{\{x \to 0\}, \{y \to \frac{1}{2}\}\}$ and $\{\{x \to \frac{3}{4}\}, \{y \to 0\}\}$ as our solutions. Then we can plot the vector field and the nullclines as depicted in Fig. 8 (a). From the nullcline analysis we can see that the solution curves will rotate around the fixed point $x = \frac{c}{d}$, $y = \frac{a}{b}$. We can continue to analyze the stability of these fixed points by determine the Jacobian matrix $J = \begin{pmatrix} 1 - 2y & -2x \\ \\ 4y & -3 + 4x \end{pmatrix}$ and its eigenvalues : for $J[0, 0]$ is $\{-3, 1\}$, and for $J[\frac{3}{4}, \frac{1}{2}]$ is $\{i\sqrt{3}, -i\sqrt{3}]\}$. Therefore the fixed point $\{0, 0\}$ is a saddle point, and $\{\frac{3}{4}, \frac{1}{2}\}$ is a center which needs to be analyzed further. Noticing that $\frac{\mathrm{d}y}{\mathrm{d}x} = (-cy + dxy)/(ax - bxy)$, we can integrate to solve it. So the analytical solution curves are given by the contours of the function $h(x, y) = x^3 y e^{-2y} e^{-4x}$ and plotted in Fig. 8 (b). The contours are actually closed curves so this proves that the orbits are periodic. We also present a contour from numerical analysis by computer simulation, and the result sketched in Fig. 8 (c) is the same compared to analytical solutions. Last, in Fig. 8 (d), we plot to show how x and y evolve as a function of time.

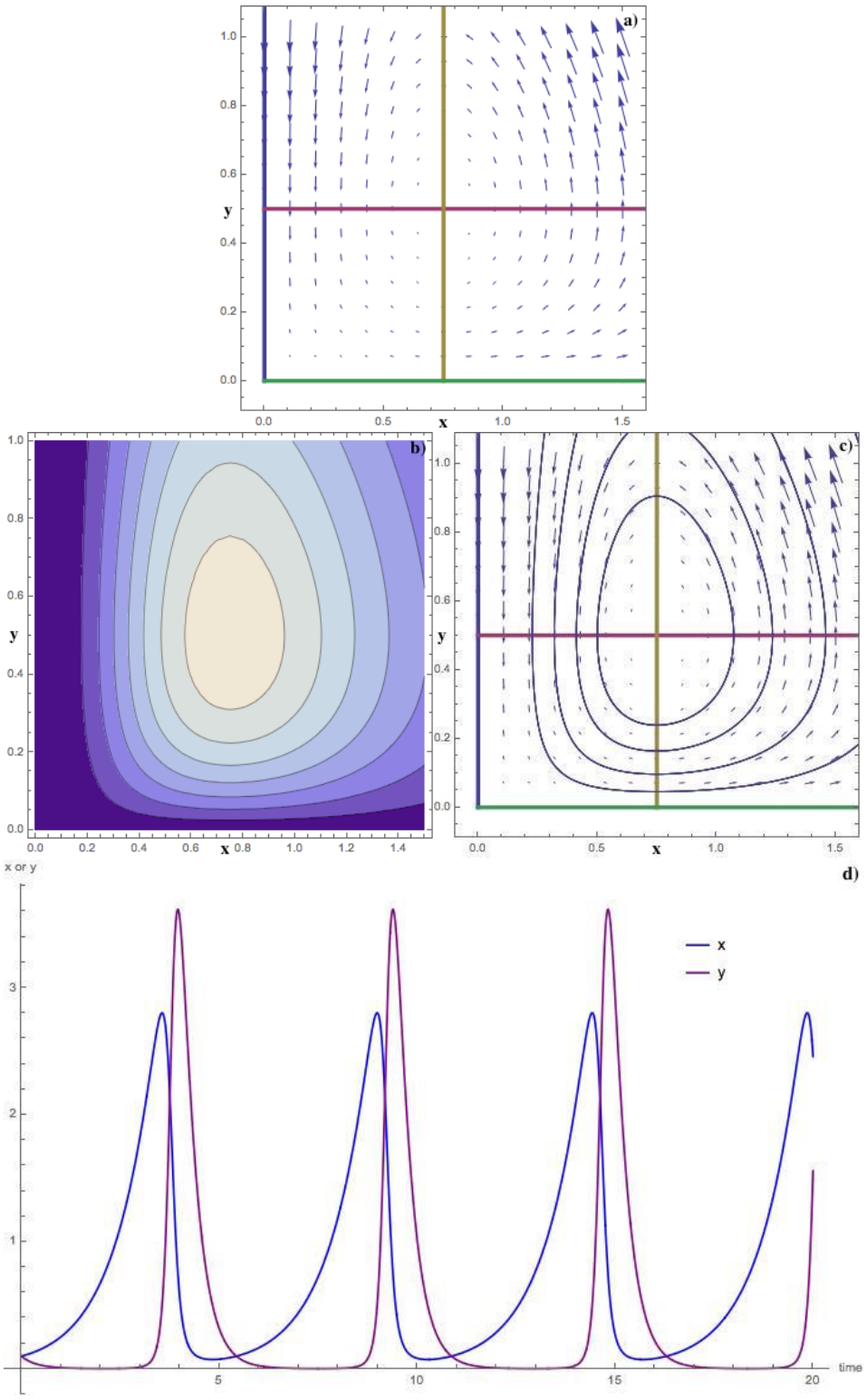

Figure 8: Nonlinear analysis of Lotka-Volterra model a) nullclines and vector field; b)contours map from analytical solution; c)contours map out from numerical solution, and d)x and y evolve as a function of time

Further inspection of Fig. 8 (d) shows that the maximum of Y always come after the maximum in X is reached. This can be explained by the mechanism itself. Returning back to the Eq. 5, step one is an autocatalytic reaction with respect to X. We can expect an increase in the production rate of X as the reaction proceeds. Then X will react with Y which refers to step two, and this is autocatalytic for Y. Thereafter, Y will increase, draining X eventually. Finally, Y will decrease to form B, which leads to a temporary depletion of Y, and also give time for X to accumulate causing the cycle to start over again. Because of this mathematical significance, this model has been employed to describe oscillation in wildlife population, economic activities, and even the spread of disease.

4.2 Brusselator Model

The first mathematical explanation of oscillating reactions was completed by I. Prigogine and G. Nicolis [28] called the Brusselator. This is a great example to show how the bifurcation theory can be applied in the analyzing the dynamics of oscillating chemical reactions. The Eq. 8. were derived from the following reactions:

$$\begin{aligned} step\ 1 &: \mathrm{A} \xrightarrow{k_1} X \\ step\ 2 &: \mathrm{B} + X \xrightarrow{k_2} Y + \mathrm{C} \\ step\ 3 &: 2X + Y \xrightarrow{k_3} 3X \\ step\ 4 &: X \xrightarrow{k_4} \mathrm{D} \\ overall &: \mathrm{A} + \mathrm{B} \rightarrow \mathrm{C} + \mathrm{D} \end{aligned} \tag{8}$$

The governing equations are obtained from the autocatalytic reaction using the law of

mass action with the dimensionless treatment of the coefficients for simplicity, the Eqn. 9 is then given by the following where x and y represent the dimensionless concentrations of two of the reactants, A and B, and a, b are dimensionless kinetic parameters.

$$\begin{aligned} \frac{\mathrm{d}x}{\mathrm{d}t} &= a - (1+b)x + yx^2 \\ \frac{\mathrm{d}y}{\mathrm{d}t} &= bx - yx^2 \end{aligned} \tag{9}$$

In the previous section, we mentioned that the dynamics analysis will sometimes be connected with Bifurcation theories. To be more specific here, we are introducing the concept of Hopf bifurcation, which is usually dealing with the birth or death of limit cycles (i.e. local periodic solutions). Wherever there exist a limit cycle, the nearby solutions will either attract forward or backward asymptotically. In this section, we mainly focused on analyzing the role of Hopf bifurcation in describing the chemical reactions. Through the same mathematical procedures as we did in analyzing Lotka-Volterra, we can obtain its single fixed point which is $\{\{x \to a\}, \{y \to \frac{b}{a}\}\}$. Then, Jacobian matrix is given by $J = \begin{pmatrix} -b-1+2xy & a^2 \\ b-2xy & a^2 \end{pmatrix}$, and at its fixed point, we have $J = \begin{pmatrix} b-1 & a^2 \\ -b & -a^2 \end{pmatrix}$. The eigenvalues of the Jacobian are given by $\lambda = \frac{(b-a^2-1) \pm i\sqrt{4a^2-(b-a^2-1)^2}}{2}$. Therefore. if $\mathrm{Re}(\lambda) < 0$ (i.e. $b < a^2+1$), this equilibrium point is an attractor otherwise it is a repeller. Given a range of parameters a and b, we plotted the stability region in parameter space as shown in Fig. 9 (a). Furthermore, by evaluating the the characteristic polynomial, we calculated the trace of the Jacobian, $\mathrm{tr}(J)$, and determinant of the Jacobian, $\det(J)$, and also we plotted the possible stability states of the Brusselator

model in terms of a and b, as seen in Fig. 9 (b). When b increases, the steady state shifts from stable node to a stable focus, then it loses its stability (i.e. the system evolves towards a limit cycle) and the steady state changes from an unstable focus to an unstable node. Also, we sketched the nullclines by setting $\dot{x} = 0$ and $\dot{y} = 0$ with some representative vectors in Fig. 9 (c) to give a global view of how x and y evolve in the trapping region. In the end, in Fig. 9 d) we provide an example to show the dynamic behavior in a phase plot through numerical integration with parameter a = 1 and b = 2.2. This simulation result is a firm justification for our analytical stability analysis. Now, we can safely claim that the system has undergone a supercritical Hopf bifurcation as we can identify that the periodic solution occurs while the equilibrium state loses its stability. Going back to Fig. 4, we can easily find that this phase portrait is exactly what the Hopf bifurcation diagram depicts when the bifurcation parameter is bigger in value that the bifurcation point, μ_c.

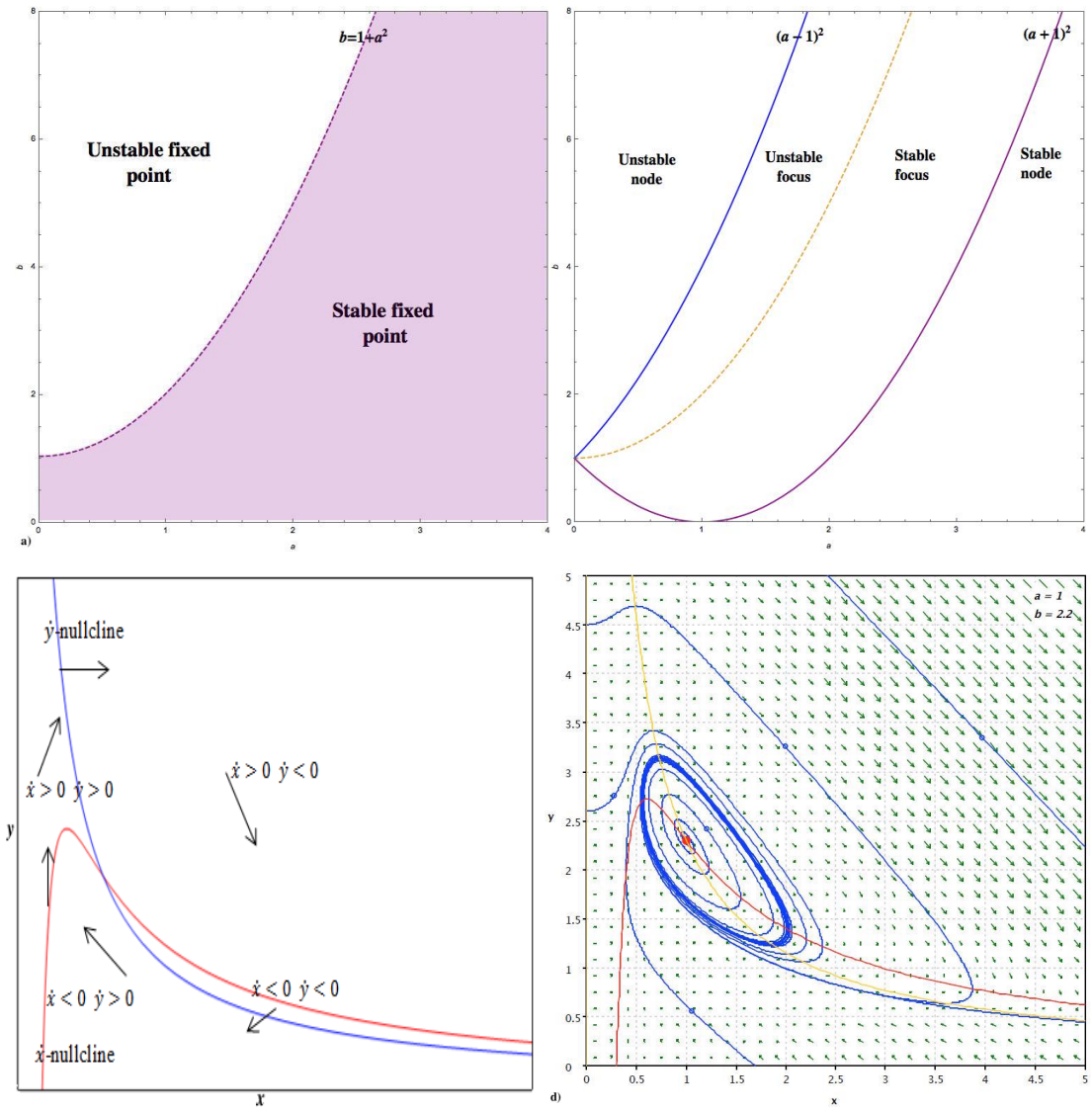

Figure 9: Stability analysis. a) Phase diagram of stability region separate the by $Re(\lambda)$; b)Stability Diagram for the Brusselator. Two solid curves are obtained by calculating the delta of characteristic polynomial. In between of these two curves, delta < 0 and > 0 otherwise; c)Nullclines and representative vectors. These vectors bound the trapping region, and d) phase plot at a=1 and b=2.2. In this case, central red equilibrium point is repeller (an unstable fixed point), and it is surrounded by a stable limit cycle. The repeller drives all the neighboring trajectories into the limit cycle. Note: the vector filed plot is a output image through a Java program, therefore the resolution may vary compared to others.

4.3 Proposed Model to Hydrogen Oxidation Reaction

4.3.1 Proposed Reaction Mechanism

The main purpose of this paper is to retain the qualitative features observed from experiments, thus we proposed a model following a L-H mechanism given by Eq. 10.

$$\begin{aligned} \mathrm{H_2} + 2* &\overset{\mathrm{k_1}}{\underset{\mathrm{k_{-1}}}{\rightleftharpoons}} 2\mathrm{H_{ad}} \\ \mathrm{O_2} + 2* &\xrightarrow{\mathrm{k_2}} 2\mathrm{O_{ad}} \\ 2\mathrm{H_{ad}} + \mathrm{O_{ad}} &\xrightarrow{\mathrm{k_3}} \mathrm{H_2O} + 3* \end{aligned} \tag{10}$$

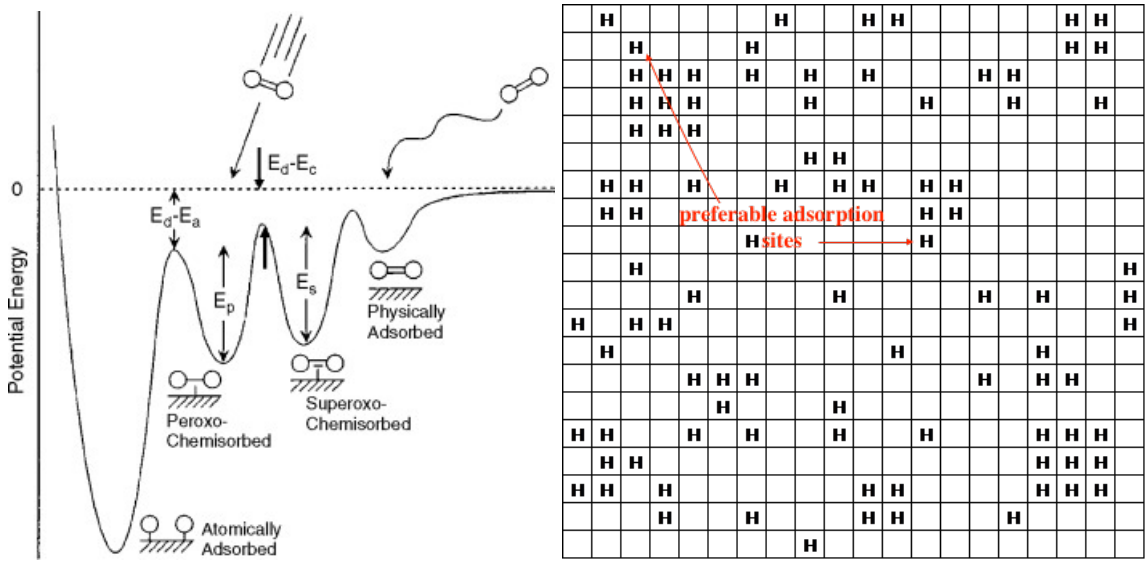

Figure 10: Left: Schematic of 1D Potential Energy and detailed dynamics for O_2 precursor-mediated dissociation on Pt(111). At high incident energies, adsorbed species can be directly excited into the molecular states (i.e. chemisorption) acting as precursors to further dissociation. While the incident energies are low, O_2 molecule first adsorbs in the physisorption well and then proceeds through sequential precursors to dissociation. Reproduced with the permission from[26]. Copyright © 2008 Elsevier B.V. All rights reserved., Right: Illustration of our proposed preferential adsorption model.

In the previous section, we have mentioned that there can be more than ten possible reactions occur on the surface, yet to include all of them seems impossible and unnecessary. Hence, we included reactions of interest. These three reactions in our model reflect the main features of the catalytic oxidation of hydrogen. A good mathematical model should be simple and describe how the adsorbed species react with each other while presenting a qualitative behavior as observed in the experiments. Here, the pathway is straightforward: firstly, the gas mixture(i.e. hydrogen and oxygen) dissociatively adsorb (i.e. chemisorption) on the platinum surface. Taking oxygen dissociation as an example, a potential energy schematic will be helpful to illustrate this dynamical process as in Fig. 10(left). Then the adsorbed species react following their stoichiometry ratio described in the third reaction. In our model, we exclude the commonly introduced reaction intermediate, hydroxyl OH [2, 27]. In the previous study, researchers found that OH can serve as a intermediate to cause autocatalysis: $\mathrm{H_2O_{ad}} + 2\mathrm{OH_{ad}} \rightarrow 3\mathrm{OH_{ad}} + 3\mathrm{H_{ad}}$. However, these model were built at a low temperature(180k or even lower), therefore the formed water molecules will stay on the surface, which is not our case. Hence, we proposed our mechanism as above.

4.3.2 Numerical Model

Based on the underlying mechanisms above, the proposed model for the oscillating kinetics is shown in Eq. 11.

$$\begin{aligned} \frac{\mathrm{d}\theta_{\mathbf{O}}}{\mathrm{d}t} &= 2k_2 P_{\mathbf{O}}(1-\theta_{\mathbf{O}}-\theta_{\mathbf{H}})^2 - k_3\theta_{\mathbf{O}}\theta_{\mathbf{H}}^2 \\ \frac{\mathrm{d}\theta_{\mathbf{H}}}{\mathrm{d}t} &= 2k_1 P_{\mathbf{H}}(1-\theta_{\mathbf{O}}-\theta_{\mathbf{H}})^2 - k_{-1}\theta_{\mathbf{H}}^2 - 2k_3\theta_{\mathbf{O}}\theta_{\mathbf{H}}^2 + k_4 P_{\mathbf{H}}\theta_{\mathbf{H}}^{0.5} \end{aligned} \tag{11}$$

Again, here we are using surface fractional coverage of adsorbed reagents to describe their surface concentrations as we introduced in the Section 2. To be specific, the adsorbed oxygen and hydrogen from the gas phase are denoted as $\theta_{\mathbf{O}}$ and $\theta_{\mathbf{H}}$, respectively. $P_{\mathbf{O}}$ and $P_{\mathbf{H}}$ are reactant-gas partial pressure. $k_i (i = 1, 2, 3, 4)$ is referred to as the rate constant of the reaction. The system displayed in Eqn. 11 has an extra term, $k_4 P_{\mathbf{H}} \theta_{\mathbf{H}}^{0.5}$, which does not belong to the reaction equations themselves. We introduced this term to describe a potential segregation of hydrogen atoms on the surface, meaning the newly adsorbed hydrogen atom is more favored to sit in the vicinity of hydrogen-occupied area. Instead of considering the details of surface diffusion driven by the surface concentration gradient, my hypothesis is that since hydrogen atoms are highly mobile compared to oxygen atoms on the catalytic terrace, it will be possible for them to migrate to the boundary of the hydrogen pre-adsorbed region after its chemisorption. Though this is a zero-dimension "point model", we tried to take a 2-dimension resolution into consideration. The power of 0.5 is due the fact that the occupied sites are proportional to the surface area which then has a square-root dependence with its available circumference to allow the newly adsorbed hydrogen atoms to sit. This idea can be described as the formation of some islands by coalescence of adsorbed atomic hydrogen. An illustration of our proposed preferential adsorption model can be seen in Fig. 10(right). Before any mathematical analysis, we hope to clarify that the oxygen adsorbed on the hydrogen island will not react with each other as this paper considers only surface species as active species.

4.3.3 Simulation Results

In this section, we provide the computational results from the model simulation. As mentioned before, the author is particularly interested in reproducing two features from experiments: 1) the oscillation arise; 2) the oscillation damp out. In order to compare the changes with the variation of different parameters, we created two sets of plots. For every different parameter, the results come as three frames of figures. Firstly, we generate a stream plot of the vector fields for two functions in Eq. 11 together with the nullclines for both $\dot{\theta}_{\mathbf{O}} = 0$(blue curve) and $\dot{\theta}_{\mathbf{H}} = 0$(red curve) in phase plane in Fig. 11. Then it is followed by a parametric plot from the data obtained by solving Eq. 11. At last, we plot to show how $\theta_{\mathbf{O}}$ and $\theta_{\mathbf{H}}$ evolve as functions of time.

dimensionless parameters	k_1	k_{-1}	k_2	k_3 **and** k_4	$P_{\mathbf{O}}$	$P_{\mathbf{H}}$	$\theta_{\mathbf{O},\,\mathrm{initial}}$	$\theta_{\mathbf{H},\,\mathrm{initial}}$
preset value	10	0.005	50	vary through case to case	0.07	0.13	0.09	0.18

Table 2: Preset parameters in the proposed model

We have tabulated the initial condition and all preset parameters using in our proposed model, as seen in Table. 2. Throughout the examination of the dynamic states of our model, we find it highly sensitive to the change of k_3 and k_4, which represent the rate constant of the third step of the reaction and hydrogen preferential adsorption, respectively. This makes sense! So the analyzing strategy is to give a range of value for k_3 and k_4, and keep the rest

fixed. It is worth noting that the real ratios between the rates of adsorption and reaction may be different.

4.3.3.1 Damped Oscillation Behavior In our first set of demonstration, we set k_4 = 10.8 and k_3 gradually increases from 2.4 to 2.7, which indicates the reaction becomes faster as the reaction proceeds, therefore the surface concentration of reactant species decrease which leads to the oscillation eventually dampening out. No obvious difference can be identified from their vector fields, as shown from Fig. 11a_1 to d_1. But we can observe this dynamic process better from the presented parametric plots from Fig. 11_a_2 to d_2. In the first frame , there is a big closed and nearly elliptical solution curve, i.e. a stable limit cycle, which gives a big stable oscillation amplitude, and then it becomes smaller when the reaction goes faster and finally the stable cycle closes up as it is attracted all the way inward to its equilibrium point wherein there exists a steady state solution. This evolution from a stable limit cycle degenerates into a central fixed point, or to be more vividly speaking, a "sink" shows the ability of this model to be dynamically versatile in qualitative description of the behavior observed experimentally.

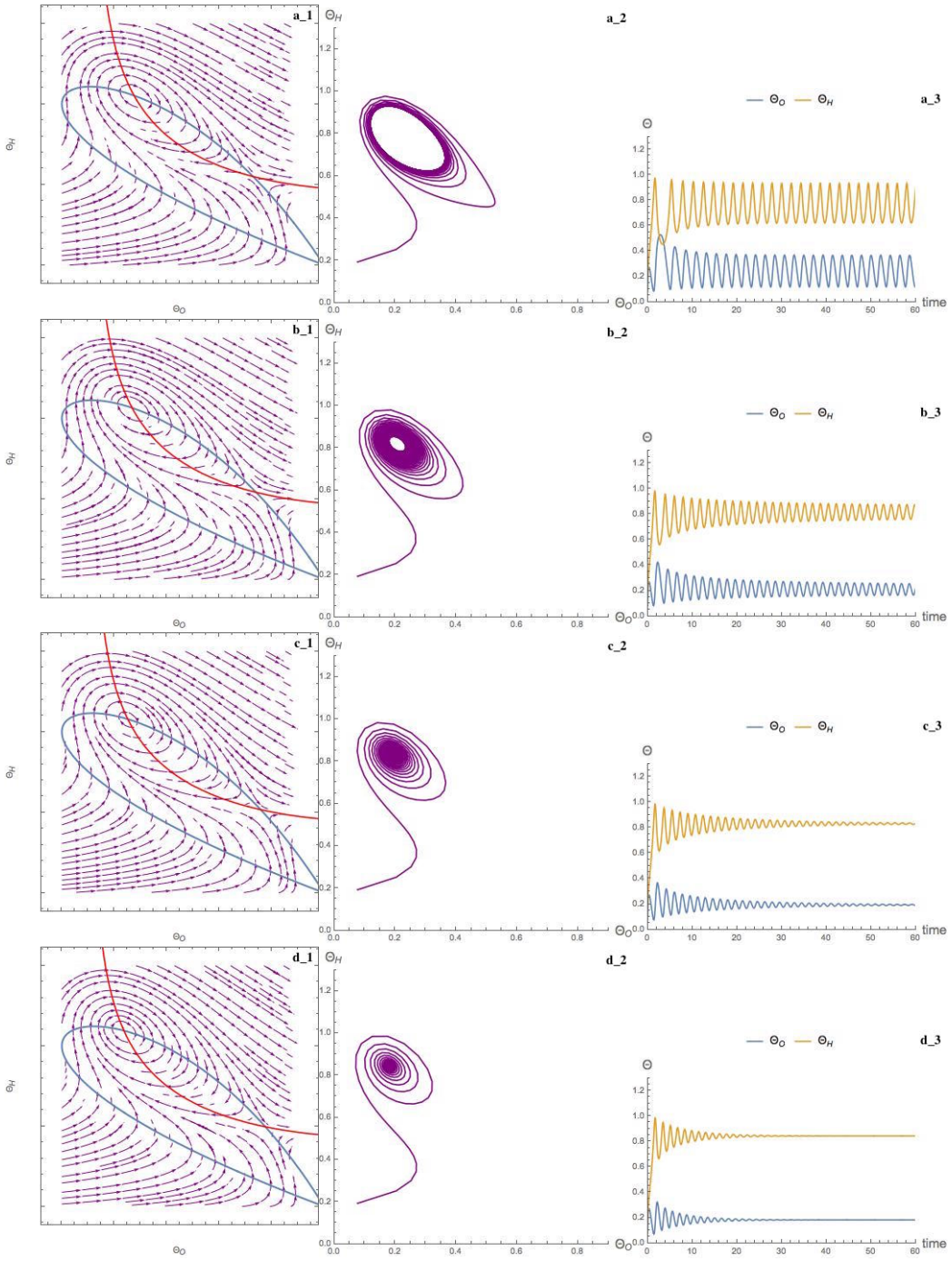

Figure 11: Diagram of system settles down to equilibrium through damped oscillation. a) k_3 = 2.4, b) k_3 = 2.5, c) k_3 = 2.55, and d) k_3 = 2.7.

4.3.3.2 Arising Oscillation Behavior Next, this set of plots shown in Fig. 12 indicates that this model has the ability to introduce an induction period before it is attracted to its oscillating region. Unlike the behavior shown in section 4.3.3.1, all trajectories spiral in to the stable fixed point eventually, here they are attracted to a gradually expanding, stable limit cycle shown from Fig. 12_a_1 to Fig. 12_d_1. With the same initial condition, we gave k_3 a constant value of 2.3, and then varied k_4 from 3.5 to 5.5. We can tell from the plots, as the hydrogen preferential adsorption rate increase, the induction period starts to decrease and the oscillation amplitude gradually increases as shown from the parameter planes. These can be attributed to growths of adsorbed hydrogen domain. As our hypothesis stated in the previous section, the preferential adsorbed atomic hydrogens are more chemically active on the surface, and this seems to push the overall reaction from on equilibrium state to another more dynamic equilibrium. As the oscillation amplitude becomes bigger, the frequency is actually getting lower. But regardless of the change of parameters, once the solution starts to oscillate, the consequent periodic behavior will go to the infinity.

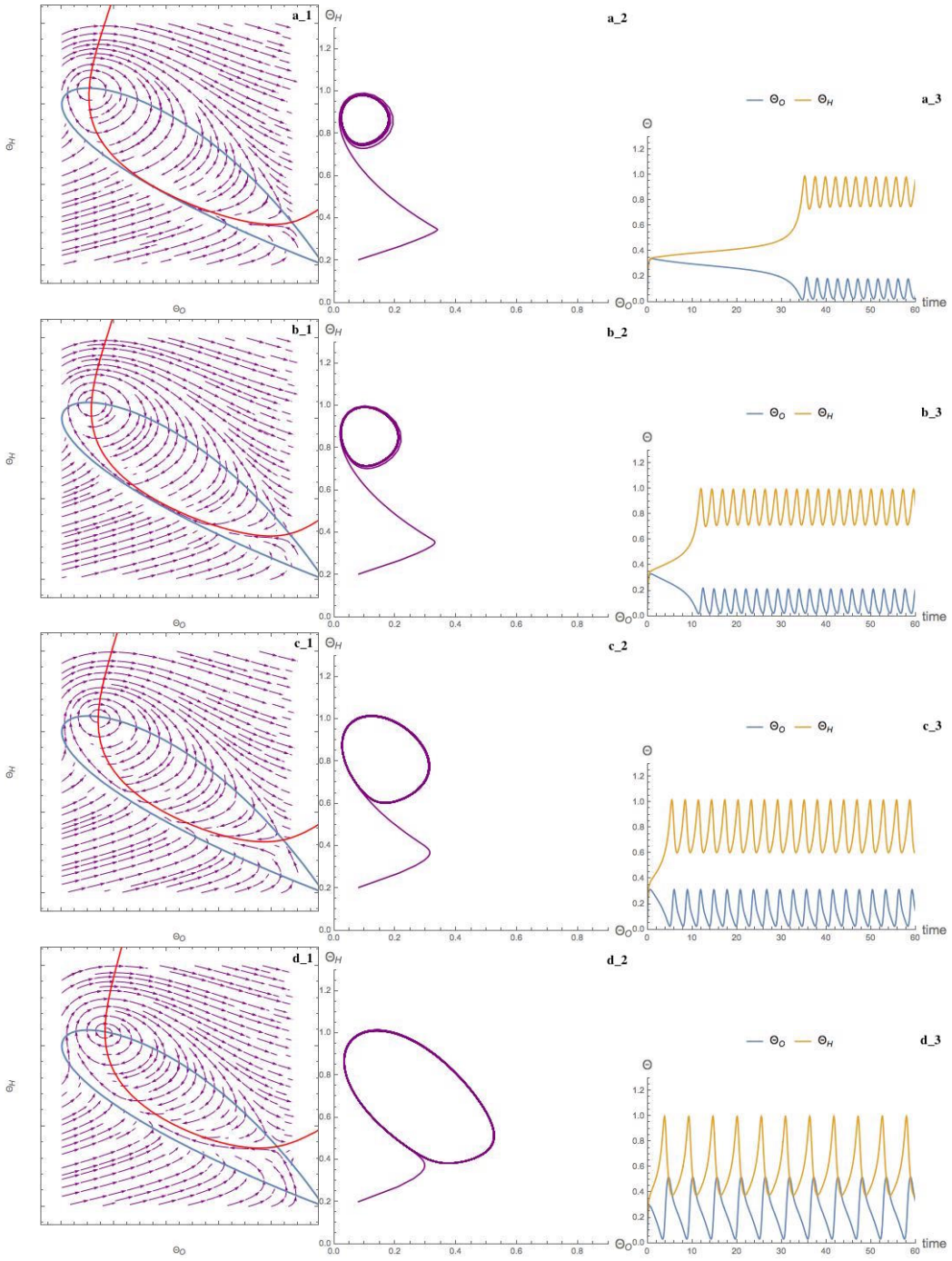

Figure 12: Diagram of system gives rise to a stable oscillation with a induction period. a) k_4 = 3.5, b) k_4 = 3.9, c) k_4 = 4.5, and d) k_4 = 5.5.

4.3.3.3 Transition from Two Steady States Above are two separate conditions representing the two features we desire to reproduce in our model. Furthermore, we have detected a much more dramatic bifurcation case. In a longer time span and given the slight variation of k_3 (from 2.75 down to 2.71) and k_4 (from 3.94 up to 3.98), we can even achieve both desired features in a single frame as shown in Fig. 13_b_3. An interesting point I would like to mention is before the oscillation occurs, the steady state surface concentration are $\theta_{\mathbf{O}} \approx 0.31$ and $\theta_{\mathbf{H}} \approx 0.36$. When it starts to oscillate, the steady state coverage will be attracted to a new fixed point which are $\theta_{\mathbf{O}} \approx 0.1$ and $\theta_{\mathbf{H}} \approx 0.88$. The trajectories jump to a distant attractor as shown from Fig. 13_b_2 to a_2. This is what we typically called subcritical bifurcation. In this case, the new attractor is a fixed point.

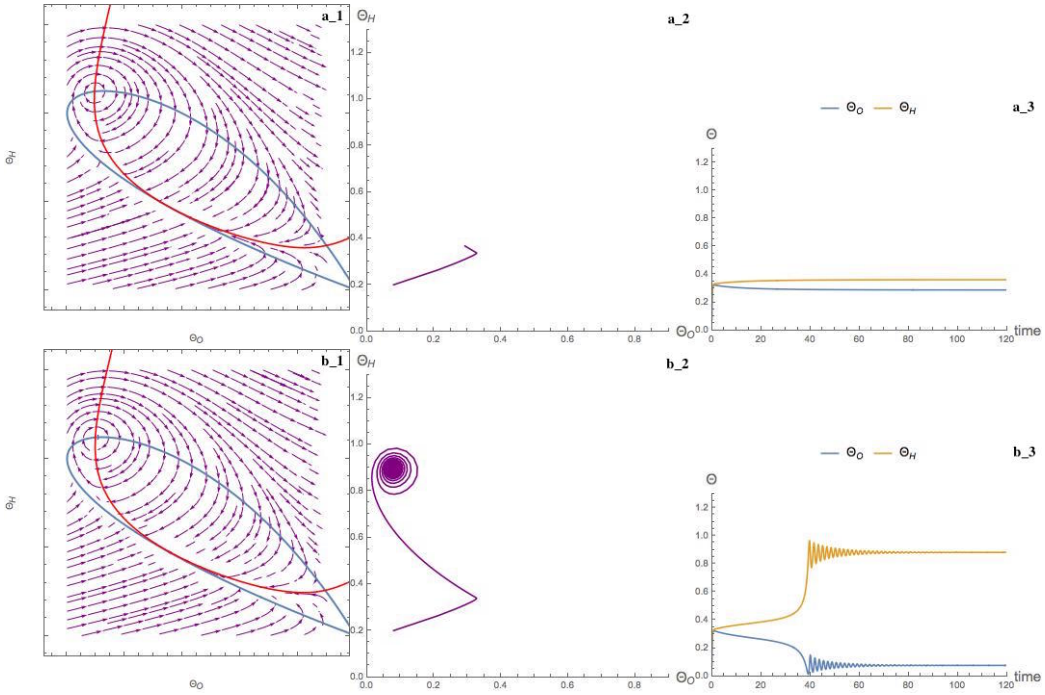

Figure 13: Diagram of system undergoes a subcritical bifurcation.

Although it seems unlikely to reproduce the whole chemicurrent profile as shown in Fig. 7,

we are able to retain some critical features with the variation of parameters in this model. In a real time situation, the rate constants are more likely dependent on the surface concentration because of the feedback mechanism in available vacancy sites, therefore they may keep changing the concentration profile of surface reactants, and this leads to the overall complex and mixed mode behavior seen in our experiments. To better understand the stability conditions, it will make sense to map out a stability phase diagram in terms of k_3 and k_4, as seen in Fig. 14. Since we don't have analytical expression for each boundary, we created a mesh with 400 points, and each point represent a set of parameters. Therefore, we can roughly generate this phase portrait with boundaries to separate individual dynamic regions. As we discussed before, the chemical process is highly dynamical and both k_3 and k_4 may change correspondingly with the variation of surface concentration profiles. Therefore a wide variety of dynamic behaviors may occur like our mixed-mode oscillation. Although k_3 and k_4 are not external parameters and they will evolve automatically within the system once the reaction starts, varying their value externally seems applicable for describing the evolution of these complex oscillating behaviors we are experiencing through experimentation, and even provides a guidance for yielding the maximum current value as this is our ultimate goal.

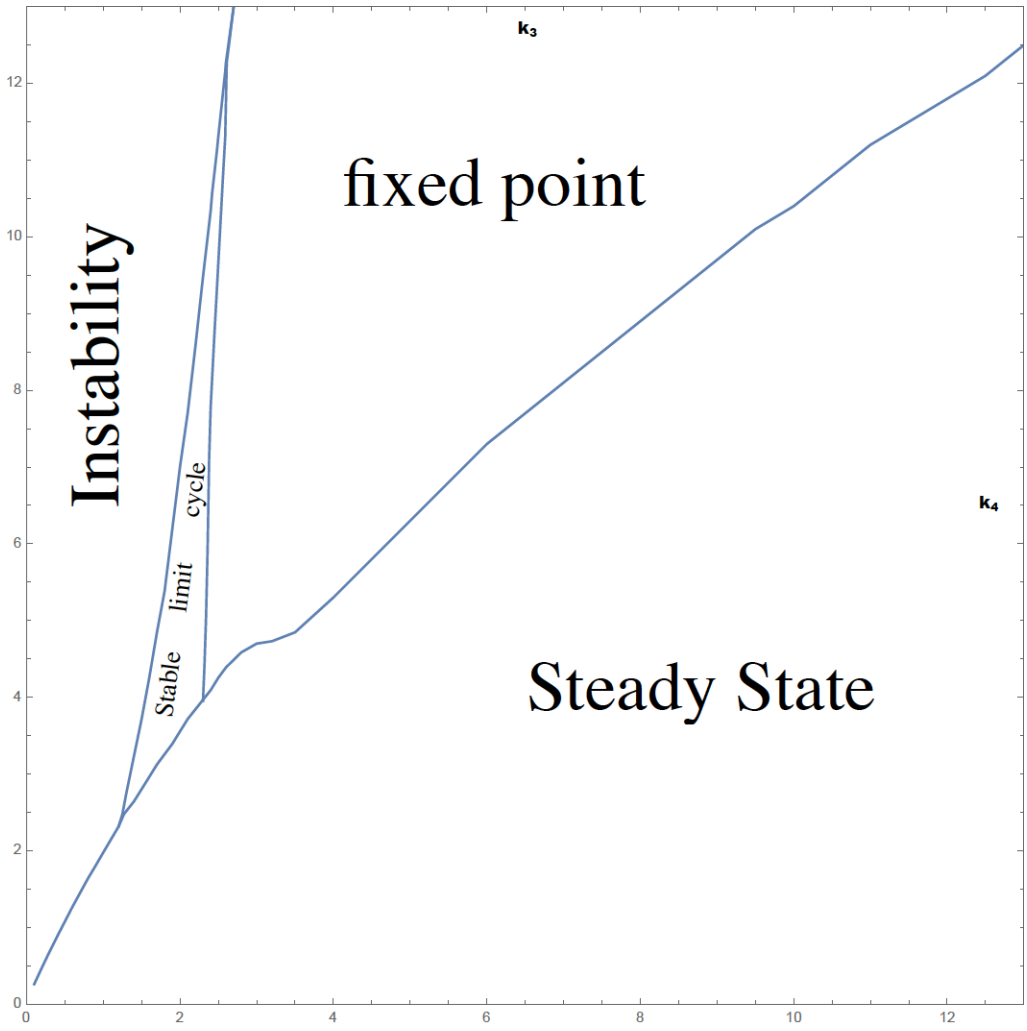

Figure 14: Stability phase diagram under the control of k_3 and k_4

5 CONCLUSION

Three chemical models were investigated. The first two give the idea of how we will perform the model analysis of a chemical oscillator. Though their models reproduce their experimental data nicely, they will not be able to describe the macroscopic behavior we observed directly. However, they provide examples to show how the stability analysis will help us understand the behaviors of a chemical system. The third one, which is our proposed model, sheds lights on a possible reaction mechanism for catalytic oxidation of hydrogen. By introducing a preferential adsorption term, $k_4 P_{\mathbf{H}} \theta_{\mathbf{H}}^{0.5}$, we brought our hypothesis that the occupancy state of adsorption site will affect the probability of adsorption and reactivity for adjacent sites. Through numerical simulation we demonstrated that our model is able to create the quintessential oscillating dynamics as we observed from experiments, moreover how the transition occurs from different states. Though, it is not a quantitative simulation, qualitative resemblances allows us some strong evidence to explain what may happen on this catalytic surface.

Of course, the author admits that the proposed model may not be the whole detailed mechanism, still it is of great importance to unveil this unusual chemicurrent behavior alongside a descriptive mathematical model. Further improvements can resort to a stochastic simulation (e.g. lattice-gas simulations based on a kinetic Monte Carlo algorithm) which will give us a more detailed, accurate description of positions of the atoms on a surface. Also, with the help with more experimental equipments (e.g. spectroscopy and $in\ situ$ microscopy), we will obtain the in situ reaction rate data, which can be further fitted into our improved model. We believe that we will be closer to the real mechanism than ever before.

References

[1] Bill Baird. Nonlinear dynamics of pattern formation and pattern recognition in the rabbit olfactory bulb. *Physica D: Nonlinear Phenomena*, 22(1-3):150–175, 1986.

[2] K. Bedürftig, S. Völkening, Y. Wang, J. Wintterlin, K. Jacobi, G. Ertl, and S. Vo. Vibrational and structural properties of OH adsorbed on Pt(111). *The Journal of Chemical Physics*, 111(24):11147, 1999.

[3] V.D. Belyaev, M.M. Slinko, M.G. Slinko, and TIMOSHEN. VI. SELF-OSCILLATION IN HETEROGENEOUS CATALYTIC REACTION OF HYDROGEN WITH OXYGEN. *DOKLADY AKADEMII NAUK SSSR*, 214(5):1098–1100, 1974.

[4] V.D. Belyaev, M.M. Slin'ko, V. Timoshenko, and M.G. Slin'ko. Onset of Oscillation in Hydrogen Oxidation on Nickel. *Kinet. Katal*, 14(3):810, 1973.

[5] V.D. Belyaev, M.M. Slin'ko, V. Timoshenko, and M.G. Slin'ko. Self-oscillations in the catalytic rate of heterogeneous hydrogen oxidation on nickel and platinum. *Kinet. Katal*, 16:555, 1975.

[6] H. Beusch, P. Fieguth, and E. Wicke. Thermisch und kinetisch verursachte Instabilitäten im Reaktionsverhalten einzelner Katalysatorkörner. *Chemie Ingenieur Technik*, pages 445–451, 1972.

[7] M. P. Cox, G. Ertl, and J. Rustig. Non-equilibrium surface phase transitions during the catalytic oxidation of CO on Pt(100). *Surface Science*, 134(2):L517–523, 1983.

[8] M. F. Cras JR. A History of the Match Industry. *J. Chem. Educ.*, 18(7):316, 1941.

[9] Daniel J. Dwyer and Friedrich M. Hoffmann. Surface science of catalysis. *American Chemical Society*, 1992.

[10] M Eiswirth and Et Al. Kinetic oscillations in the catalytic CO oxidation on a Pt(110) surface. *Surface Science*, 177(1):90–100, 1986.

[11] M. Eiswirth, K. Krischer, and G. Ertl. Transition to chaos in an oscillating surface reaction. *Surface Science*, 202(3):565–591, 1988.

[12] M. Eiswirth, P. Moller, K. Wetzl, R. Imbihl, and G. Ertl. Mechanisms of spatial self-organization in isothermal kinetic oscillations during the catalytic CO oxidation on Pt single crystal surfaces. *The Journal of Chemical Physics*, 90(1):510, 1989.

[13] T. Engel and G Ertl. Elementary steps in the catalytic oxidation of carbon monoxide on platinum metals. *Advances in Catalysis 28 (1979): 1-78.*, (28):1–78, 1979.

[14] G Ertl. Nonlinear Dynamics: Oscillatory Kinetics and Spatio-Temporal Pattern Formation. In *Handbook of Heterogeneous Catalysis*, volume 3, pages 1492–1516. Wiley-VCH Verlag GmbH & Co. KGaA., 2nd edition, 2008.

[15] Richard J. Field and F. W. Schneider. Oscillating chemical reactions and nonlinear dynamics. *Journal of Chemical Education*, 66(3):195, 1989.

[16] N. Freyer, M. Kiskinova, and H. P. Bonzel. Oxygen adsorption on Pt(110)-(1×2) and Pt(110)-(1×1). *Surface Science*, 166:206–220, 1986.

[17] S.A. Gourley, J.W. So, and J.H. Wu. Nonlocality of Reaction-Diffusion Equations Induced by Delay: Biological Modeling and Nonlinear Dynamics. *Journal of Mathematical Sciences*, 124(4):5119–5153, 2004.

[18] John Guckenheimer and Philip Holmes. *Nonlinear oscillations, dynamical systems, and bifurcations of vector fields*, volume 42. Springer Science & Business Media, New York, 1983.

[19] Mohammad A. Hashemian, Suhas K. Dasari, and Eduard G. Karpov. Separation of hot electron current component induced by hydrogen oxidation on resistively heated Pt/n-GaP Schottky nanostructures. *Journal of Vacuum Science & Technology A: Vacuum, Surfaces, and Films*, 31(2):20603, 2013.

[20] B. Hellsing, B. Kasemo, and V. P. Zhdanov. Kinetics of the hydrogen-oxygen reaction on platinum. *Journal of Catalysis*, 132(1):210–228, 1991.

[21] M. Hildebrand. Self-organized nanostructures in surface chemical reactions: Mechanisms and mesoscopic modeling. *Chaos*, 12(1):144–156, 2002.

[22] R. Imbihl. Chapter 9 Non-linear Dynamics in Catalytic Reactions. *Dynamics*, Volume 3(08):341–428, 2008.

[23] R. Imbihl and G. Ertl. Oscillatory Kinetics in Heterogeneous Catalysis. *Chemical Reviews*, 95(3):697–733, 1995.

[24] N. M. H. Janssen, P. D. Cobden, and B. E. Nieuwenhuys. Non-linear behaviour of nitric oxide reduction reactions over metal surfaces. *J. Phys.: Condens. Matter*, 9:1889–1917, 1997.

[25] Alfred J. Lotka. Contribution to the Theory of Periodic Reactions. *J. Phys. Chem.*, 3(14):271–274, 1910.

[26] A. C. Luntz. The Dynamics of Making and Breaking Bonds at Surfaces. In *Chemical Bonding at Surfaces and Interfaces*, pages 143–254. Elsevier B.V., 2008.

[27] A. Michaelides and P. Hu. Catalytic Water Formation on Platinum : A First-Principles Study. *J. Am. Chem. Soc.*, 123(18):4235–4242, 2001.

[28] Gregoire Nicolis, Ilya Prigogine, and Et Al. *Self-organization in nonequilibrium systems*, volume 19. Wiley, New York, 1977.

[29] H. Nienhaus. Electronic excitations by chemical reactions on metal surfaces. *Surface Science Reports*, 45:1, 2002.

[30] H. Nienhaus, H. S. Bergh, B. Gergen, a. Majumdar, W. H. Weinberg, and E. W. McFarland. Ultrathin Cu films on Si(111): Schottky barrier formation and sensor applications. *Journal of Vacuum Science & Technology A: Vacuum, Surfaces, and Films*, 17(4):1683, 1999.

[31] H. Nienhaus, B. Gergen, W. H. Weinberg, and E. W. McFarland. Detection of chemically induced hot charge carriers with ultrathin metal film Schottky contacts. *Surface Science*, 514(1-3):172–181, 2002.

[32] J. Y. Park, J. R. Renzas, B. B. Hsu, and G. A. Somorjai. Interfacial and Chemical Properties of Pt/TiO2, Pd/TiO2, and Pt/GaN Catalytic Nanodiodes Influencing Hot Electron Flow. *Journal of Physical Chemistry C*, 111(42):15331–15336, 2007.

[33] C. Sachs, M. Hildebrand, S. Volkening, J. Wintterlin, and G. Ertl. Spatiotemporal self-organization in a surface reaction: from the atomic to the mesoscopic scale. *Science*, 293(5535):1635–1638, 2001.

[34] F. Schüth, B. E. Henry, and L. D. Schmidt. Oscillatory reactions in heterogeneous catalysis. *Advances in Catalysis*, 39:51–127, 1993.

[35] M. Sheintuch and H. A. Schmitz. Oscillations in catalytic reactions. *Catalysis Reviews Science and Engineering*, 15(1):107–172, 1977.

[36] M. M. Slinko and N. I. Jaeger. Oscillatory behaviour in the oxidation of CO. *Oscillating Heterogeneous Catalytic Systems*, (86):47–120, 1994.

[37] S. H. Strogatz. *Nonlinear dynamics and chaos: with applications to physics, biology, chemistry, and engineering*. Westview press, 2014.

[38] A. M. Turing. The chemical basis of morphogenesis. *Philosophical Transactions of the Royal Society of London B: Biological Sciences*, 237(641):37–72, 1952.

[39] S. Völkening, K. Bedürftig, K. Jacobi, J. Wintterlin, and G. Ertl. Dual-Path Mechanism for Catalytic Oxidation of Hydrogen on Platinum Surfaces. *Physical Review Letters*, 83(13):2672–2675, 1999.

[40] W. R. Williams, C. M. Marks, and L. D. Schmidt. Steps in the Reaction H2 + O2 <–> H2O on Pt: OH Desorption at High Temperatures. *The Journal of Physical Chemistry*, 96:5922–5931, 1992.

[41] A. T. Winfree. Rotating chemical reactions. *Scientific American*, 230:82–95, 1974.

[42] Yong Yao and Walter J. Freeman. Model of biological pattern recognition with spatially chaotic dynamics. *Neural Networks*, 3(2):153–170, 1990.

[43] M. P. Zum Mallen, W. R. Williams, and L. D. Schmidt. Steps in Hydrogen Oxidation on Rhodium: Hydroxyl Desorption at High Temperatures. *The Journal of Physical Chemistry*, 97(3):625–632, 1993.

VITA

NAME: Songyun Liu

EDUCATION: B.Eng., Metal Materials Engineering, Hefei University of Technology, Hefei, 2012

PUBLICATION: Qi, W., Liu, W., Liu, S., Zhang, B., Gu, X., Guo, X., and Su, D. (2014). Heteropoly Acid/Carbon Nanotube Hybrid Materials as Efficient SolidAcid Catalysts.ChemCatChem, 6(9), 2613-2620.,